G. R. ABRAHAMSON

Director,
Poulter Laboratory,
Stanford Research Institute,
Menlo Park, Calif.
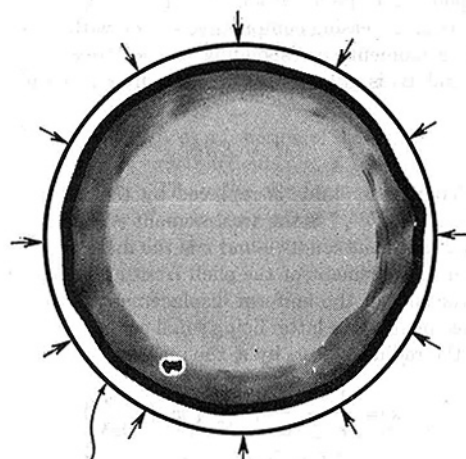
Critical Velocity for Collapse of a Shell of Circular Cross Section Without Buckling

Many practical devices involve high-speed collapse of shells of circular cross section. In all of the devices the stability of the collapse motion is of interest and in some it is essential for successful operation. In this paper, the buckling motion of shells of circular cross section during high-speed collapse is analyzed and critical collapse velocities are determined for which the growth of initial nonuniformities by buckling during collapse is 10 and 100.

Introduction

HIGH-SPEED collapse of shells of circular cross section occurs in many practical devices. Examples are explosive closure devices for obtaining gastight pipe seals in tens of microseconds, magnetic-field constriction devices for producing intense transient magnetic fields, shock tubes driven by rapidly collapsing a cylindrical reservoir to produce transient gas flows with very high pressures and velocities, and armor-piercing rounds and oil-well perforating devices using rapidly collapsing conical shells to produce metallic jets that travel at velocities of the order of 10,000 fps. In all these examples the stability of the shell as it collapses is of interest and in some cases it is critical to successful operation.

As shown in Fig. 1(a), buckling occurs in shells of circular cross section projected inward at initial velocities sufficient to produce moderate permanent deformation ($\sim$10 percent). It has been shown [1, 2][1] that this type of buckling develops from nonuniformities that grow exponentially with time during the inward motion. As indicated in Fig. 1(b), the compressive hoop stress that develops during collapse causes nonuniformities to grow; i.e., elements that lag the average motion are thrust farther behind, and those that lead are thrust farther ahead. Since growth to significant magnitudes requires time, and since the shell becomes more stable as it becomes thicker, at sufficiently high collapse velocities the buckling will be negligible. Hence, a

---

[1] Numbers in brackets designate References at end of paper.

Fig. 1(a) Typical buckled shape of circular cylindrical aluminum (2024-T3) shell subjected to an inward radial impulse

ORIGINAL DIA. 2.99 in. 780 ft/sec
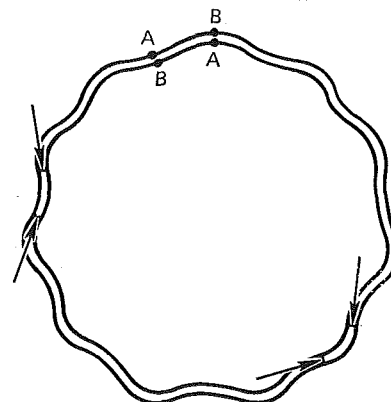(WALL 0.076, LENGTH 6)   CYL. NO. 23

Fig. 1(b) Tendency of imperfections to grow under compressive hoop stress
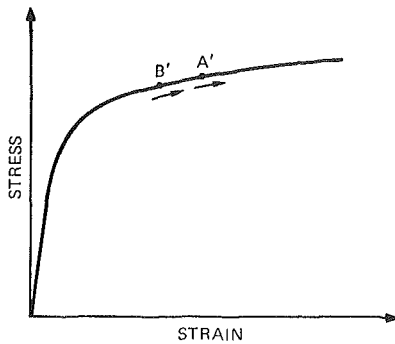
Fig. 2 Stress-strain curve

Fig. 3 Notation

critical collapse velocity (constant or nonuniform) can be determined for which the growth during collapse does not exceed a specified magnitude. In the present paper, the analysis of [1] is extended to determination of the growth of initial nonuniformities in shape for constant collapse velocity.

Differential Equation

Since we are concerned with small buckling displacements, we may take the flexural strain rate to be less than the hoop strain rate, so the strain in the shell during inward motion always increases. At points A in Fig. 1(b), the flexural strain rate adds to the compressive hoop strain rate and at points B it subtracts from it. Then on the stress-strain curve in Fig. 2, points A' and B', corresponding to points A and B in Fig. 1(b), always move in the direction of increasing compressive strain, with A' leading B'. The bending moment corresponding to the stress difference between A' and B' is given approximately by the simple formula for a bar

$$M = E_t I \kappa \tag{1}$$

in which Young's modulus is replaced by the tangent modulus E_t between A' and B', I is the area moment of inertia of the cross section (per unit axial length), and κ is the increase in curvature. The inward displacement of the shell from an initial radius a is taken as the sum of the uniform displacement w_0 and the buckling displacement w, the latter being small compared to the radius. Denoting the radius $a - w_0$ by r, the increase in curvature is

$$\kappa = \frac{1}{r} - \frac{1}{a} + \frac{1}{r^2}\left(w + \frac{\partial^2 w}{\partial \theta^2}\right) \tag{2}$$

This expression neglects the curvature change due to initial nonuniformities, an approximation that doesn't significantly affect the results of the present investigation.

The equation of motion for an element of a collapsing shell is readily found with the aid of Fig. 3. Neglecting rotational inertia, we have for the shear force (per unit axial length)

$$Q = \frac{\partial M}{\partial \lambda} \tag{3}$$

$d\lambda$ being the arc length corresponding to $d\theta$ and subtending the angle $d\phi$ at the instantaneous center of curvature. Denoting compressive hoop stress by σ, wall thickness by h, density by ρ, and external pressure by P, we find for the radial motion

$$\frac{\partial Q}{\partial \lambda} + \sigma h \frac{\partial \phi}{\partial \lambda} - P = \rho h \frac{\partial^2}{\partial t^2}(r - w) \tag{4}$$

The curvature is

$$\frac{\partial \phi}{\partial \lambda} = \frac{1}{a} + \kappa_i + \kappa \tag{5}$$

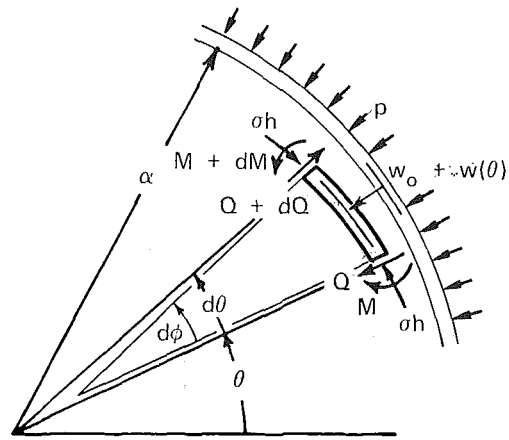where κ_i is the curvature due to a small initial departure from

circularity and, as indicated in (2), κ is the increase in curvature. Denoting the initial departure from circularity by w_i, we have for the curvature at any instant due to the initial displacement

$$\kappa_i = \frac{1}{r^2}\left(w_i + \frac{\partial^2 w_i}{\partial \theta^2}\right) \tag{6}$$

Substituting (6) and (2) into (5) and the result into (4), and eliminating Q using (3) and M using (1) and (2), with $I = h^3/12$ and $d\lambda = rd\theta$, we obtain for the differential equation for the displacements

$$\frac{E_t}{12} \frac{h^3}{r^4}\left(\frac{\partial^4 w}{\partial \theta^4} + \frac{\partial^2 w}{\partial \theta^2}\right) + \sigma h \left[\frac{1}{r} + \frac{1}{r^2}\left(w + \frac{\partial^2 w}{\partial \theta^2}\right)\right.$$
$$\left. + \frac{1}{r^2}\left(w_i + \frac{\partial^2 w_i}{\partial \theta^2}\right)\right] = \rho h \frac{\partial^2}{\partial t^2}(r - w) + P. \tag{7}$$

In the absence of initial imperfections and buckling, (7) reduces to

$$\frac{\sigma h}{r} = \rho h \frac{\partial^2 r}{\partial t^2} + P. \tag{8}$$

For collapse at constant velocity, (8) becomes simply

$$\frac{\sigma h}{r} = P \tag{9}$$

as expected. Hence, for collapse at constant velocity (7) becomes

$$\frac{E_t}{12} \frac{h^2}{r^4}\left(\frac{\partial^4 w}{\partial \theta^4} + \frac{\partial^2 w}{\partial \theta^2}\right) + \frac{\sigma}{r^2}\left[\left(w + \frac{\partial^2 w}{\partial \theta^2}\right) + \left(w_i + \frac{\partial^2 w_i}{\partial \theta^2}\right)\right]$$
$$= -\rho \frac{\partial^2 w}{\partial t^2}. \tag{10}$$

Denoting the initial wall thickness by h_0, from continuity we have the approximate relation

$$h = h_0 \frac{a}{r}. \tag{11}$$

Also, letting

$$\beta = \frac{E_t}{E_0}, \qquad \gamma = \frac{\sigma}{\sigma_0} \tag{12}$$

where E_0 and σ_0 are reference values, introducing the dimensionless quantities

$$s^2 = 12 \frac{\sigma_0}{E_0}\left(\frac{a}{h_0}\right)^2, \qquad T^2 = 12 \frac{a^4}{h_0^2} \frac{\rho}{E_0} \tag{13}$$

and putting $\alpha = r/a$, $\tau = t/T$, equation (10) becomes

$$\beta(w'''' + w'') + s^2\gamma\alpha^4[(w + w'') + (w_i + w_i'')] = -\alpha^6\ddot{w}$$

(14)

where

$$(\quad)' = \partial(\quad)/\partial\theta \text{ and } (\dot{\ }) = \partial^2(\quad)/\partial\tau^2.$$

Finally, writing $u = w/a$ and rearranging terms, (14) becomes

$$\alpha^6\ddot{u} + s^2\gamma\alpha^4 u + (\beta + s^2\gamma\alpha^4)u'' + \beta u''''$$
$$= -s^2\gamma\alpha^4(u_i + u_i'') \quad (15)$$

For $\alpha = 1$, $\beta = 1$, and $\gamma = 1$, (15) corresponds to equation (10) of [1], except that a term $-s^2$ is missing from the right-hand side due to the constant collapse velocity used in the present analysis.

Critical Collapse Velocity

Since the differential equation (15) is linear, we may take for the buckling displacement

$$u = \sum_{n=2}^{\infty} [F_n(\tau) \cos n\theta + G_n(\tau) \sin n\theta] \quad (16)$$

and for the initial departure from circularity

$$u_i = \sum_{n=2}^{\infty} [A_n \cos n\theta + B_n \sin n\theta] \quad (17)$$

the terms for $n = 1$ being omitted because they do not contribute to the buckling motion. Substituting (16) and (17) into (15) yields

$$\alpha^6\ddot{F}_n + [s^2\gamma\alpha^4 - n^2(\beta + s^2\gamma\alpha^4) + \beta n^4]F_n$$
$$= -s^2\gamma\alpha^4(1 - n^2)A_n \quad (18)$$

and a similar equation for G_n. Dividing by A_n and putting $f_n = F_n/A_n$, (18) becomes

$$\alpha^6\ddot{f}_n + (n^2 - 1)(\beta n^2 - s^2\gamma\alpha^4)f_n = s^2\gamma\alpha^4(n^2 - 1) \quad (19)$$

The nature of the buckling motion is apparent from (19). For negative values of the coefficient of f_n, the solutions are hyperbolic functions and the magnitude of f_n grows exponentially with time. Taking $\beta = 1$ and $\gamma = 1$ initially, and noting that $\alpha = 1$ at the beginning of the motion, we see that modes with $n^2 < s^2$ are initially unstable. As collapse proceeds, α decreases; hence at some point the coefficient of f_n becomes positive and the modes that were initially unstable become stable, i.e., they become oscillatory. However, while α decreases during collapse, in general γ increases and β decreases. Thus the growth during the period of instability depends not only on the rate of collapse, but also on the shape of the stress-strain curve.

To integrate (19) we must know α as a function of τ, and we must know β and γ as functions of strain and hence of α. Instead of solving (19) for any particular material, in this paper we obtain the critical collapse velocity for $\beta = 1$ and $\gamma = 1$. This corresponds to a hypothetical rigid linear-strain-hardening material ($\beta = 1$) with a small hardening modulus ($\gamma = 1$).

For a constant collapse velocity V,

$$\alpha = \frac{r}{a} = \frac{a - w_0}{a} = 1 - \frac{w_0}{a} = 1 - \frac{Vt}{a}.$$

In terms of τ this may be written

$$\alpha = 1 - q\tau \quad (20)$$

where

$$q = T'\frac{V}{a} = \sqrt{12}\,\frac{a}{h_0}\,\frac{V}{\sqrt{\frac{E_0}{\rho}}} = s\frac{V}{\sqrt{\frac{\sigma_0}{\rho}}} \quad (21)$$
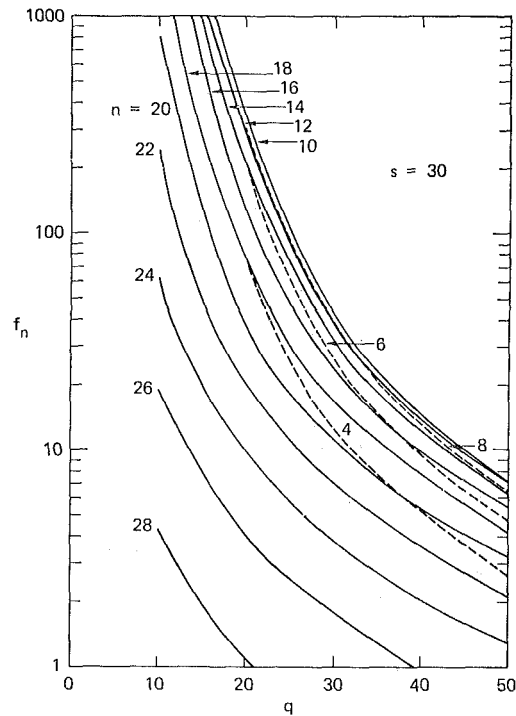

Fig. 4 Final magnitude of f_n for $s = 30$; critical mode is $n = 10$

Using (20) and the initial conditions $f_n = \dot{f}_n = 0$, (19) was integrated numerically for values of $n < s$. The final magnitude of f_n was taken as the magnitude just prior to the change in sign of the coefficient of f_n in (19).

The final magnitude of f_n as a function of n and q, for $s = 30$, is shown in Fig. 4. For any particular n, f_n decreases with increasing q, as expected. The value of n for which f_n is maximum is $n = 10$. The value of α at the instant the mode $n = 10$ becomes stable is found from the coefficient of f_n in (19) and, with $\beta = \gamma = 1$, is given by

$$\alpha = \sqrt{\frac{n}{s}} \quad (22)$$

For $s = 30$ and $n = 10$, $\alpha = 0.577$.

Curves such as those in Fig. 4 were calculated for $15 \leq s \leq 200$. From these curves, the values of q for $f_n = 10$ and $f_n = 100$ were determined and are shown in Fig. 5 along with the critical mode numbers. For a particular value of s, the critical velocity q is greater for $f_n = 10$ than for $f_n = 100$, as expected. Also, for thinner shells, i.e., larger values of s, the critical velocity increases. The critical mode numbers increase with s, but are nearly the same for both curves for the same value of s.

To determine the critical collapse velocity for a particular example, we proceed as follows. From (13) and (21), we have

$$s = \sqrt{12}\,\sqrt{\frac{\sigma_0}{E_0}}\,\frac{a}{h_0}, \qquad q = \sqrt{12}\,\frac{a}{h_0}\,\frac{V}{\sqrt{\frac{E_0}{\rho}}} \quad (23)$$

We see that geometry enters both of these expressions only through the radius-to-thickness ratio. However, material properties affect s through the ratio of the flow stress σ_0 to the slope E_0 of the stress-strain curve, and they affect q through the velocity $(E_0/\rho)^{1/2}$. A reasonable value for $(\sigma_0/E_0)^{1/2}$ is 0.5, and a reasonable value for $(E_0/\rho)^{1/2}$ is 5×10^4 cm/sec. Then, taking $a/h_0 = 30$, we find
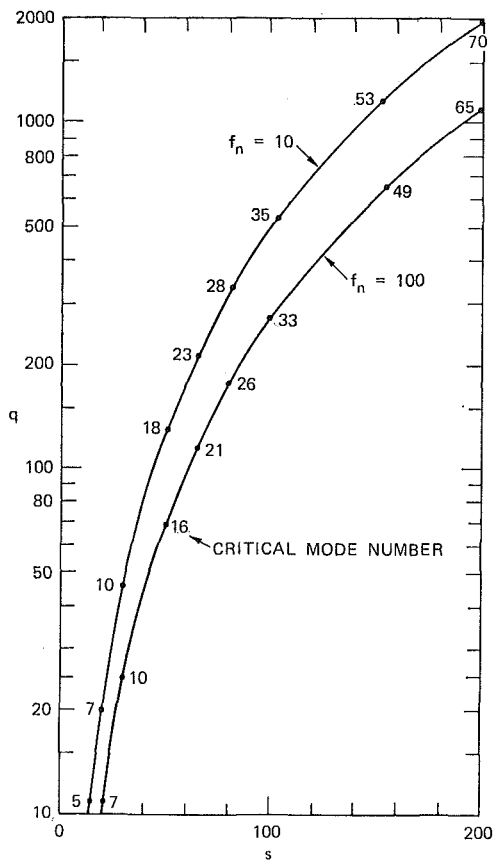
$$s = \sqrt{12}(0.5)30 = 52.$$

Fig. 5 Critical collapse velocity curves for $f_n = 10$ and 100

From the curve for $f_n = 10$ in Fig. 5, we find $q = 130$ for $s = 52$. Then, from (23), we have for V

$$V = q \frac{h_0}{a} \frac{\sqrt{E_0/\rho}}{\sqrt{12}} = 130 \frac{1}{30} \frac{5 \times 10^4}{\sqrt{12}}$$

$$V = 6.2 \times 10^4 \text{ cm/sec} = 0.6 \text{ mm/}\mu\text{sec} = 1800 \text{ fps}.$$

Direct experimental evidence is lacking to check the results of the preceding analysis. However, collapse velocities for copper shaped-charge liners are in the range of 1 mm/μsec (3300 fps), in qualitative agreement with the foregoing result. To make a quantitative verification of the theory, actual stress-strain curves should be used in the numerical integration of (19).

Discussion

In the foregoing analysis, we used a simple uniaxial stress-strain law, Fig. 2. Here we discuss the bending resistance of a collapsing shell using a biaxial law.

We take the radial stress through the shell thickness to be zero. Then the von Mises yield condition in terms of the principal stresses σ_θ (hoop stress) and σ_x (axial stress) is as shown in Fig. 6(a). Taking the principal axes of the plastic strain increment to be parallel to the axes of the principal stresses (Reuss flow rule), the axes in Fig. 6(a) are also the axes of the principal plastic strain increments $\Delta\epsilon_\theta$ and $\Delta\epsilon_x$. For a shell projected radially inward with no axial strain, σ_θ is compressive and $\Delta\epsilon_x = 0$. Thus the corresponding point on the yield ellipse is point 0 in Fig. 6(a), at which σ_θ is compressive and the normal to the yield ellipse (which gives the direction of the plastic strain increment vector) is parallel to the $\Delta\epsilon_\theta$-axis.

For a material that strain hardens isotropically, the yield ellipse expands as the strain increases. If buckling occurs as shown in Fig. 1(b), the hoop strain at A will be greater than that
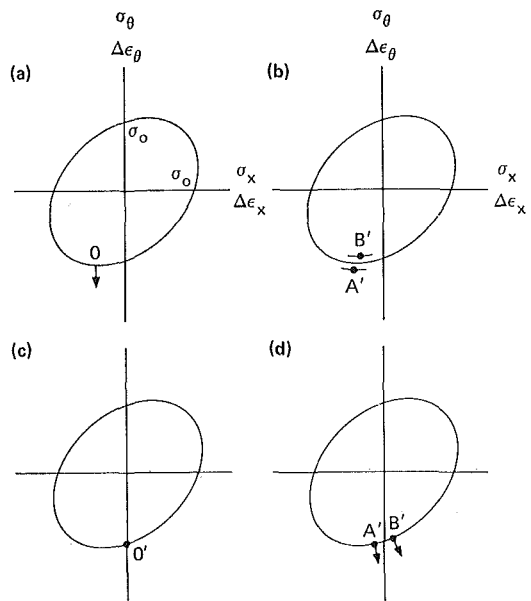

Fig. 6 Biaxial stress states of collapsing shells on the von Mises yield ellipse

at B. Hence, as shown in Fig. 6(b), the corresponding stresses will lie on expanding yield ellipses on either side of the expanding yield ellipse corresponding to the average hoop strain. The difference in σ_θ between A' and B' implies a bending moment that resists the buckling motion. Since this moment is due to strain hardening, it is called the strain-hardening moment. The foregoing analysis is based on bending resistance due to the strain-hardening moment.

Strain-rate effects can also give rise to bending moments that resist the buckling motion. From Fig. 1(b) it is apparent that the hoop strain rate at A exceeds that at B. Hence, if the yield stress of the material increases with strain rate, the stresses corresponding to A and B will lie on yield ellipses on either side of the yield ellipse corresponding to the average hoop strain rate, analogous to the situation with strain hardening, Fig. 6(b). Florence [3] has analyzed the buckling of strain-rate sensitive mild steel cylinders.

For a material for which strain hardening is independent of strain rate, the critical collapse velocity based on strain hardening alone is an upper bound. However, for a material for which strain hardening decreases with increasing strain rate, a more complete analysis than that given in this paper is required to determine a critical collapse velocity.

If instead of $\Delta\epsilon_x = 0$ we have $\sigma_x = 0$ (as for a ring), the corresponding point on the yield ellipse for a shell that collapses without buckling is 0' in Fig. 6(c). If buckling occurs, the hoop strain at A, Fig. 1(b) will be greater than the average and that at B will be less, but the axial strain will be the same at A and B. Thus the strain increment vectors corresponding to points A and B have the same axial component but different hoop components. Hence, the direction of the strain increment vectors for A and B will not be parallel to that at 0' in Fig. 6(c), but will be shifted slightly. Since the strain increment vectors must be normal to the yield ellipse, the difference in the direction of the strain increment vectors implies a stress difference at A and B as indicated in Fig. 6(d). The bending moment due to this stress difference Goodier has termed the directional moment. It is interesting to note that directional moments do not arise for $\Delta\epsilon_x = 0$, since all strain increment vectors are in the same direction. Florence and Goodier [4] analyzed the axisymmetric buckling of thick-walled tubes including the effects of directional moments.

In high-speed collapse of cylindrical shells, the resistance to buckling must come initially from strain-hardening and strain-

rate moments, since the axial flow required for the development of directional moments can occur only in the material that has been reached by relief waves from the ends of the shell. Since shells become thicker and hence more stable as they collapse, the most important part of the buckling occurs in the initial stages of collapse. Hence, in many problems, directional moments may be unimportant. Moreover, the increased bending resistance due to directional moments tends to decrease the critical collapse velocity. Hence, a critical collapse velocity calculated without regard to directional moments is an upper bound.

Acknowledgments

References

1 Abrahamson, G. R., and Goodier, J. N., "Dynamic Plastic Flow Buckling of a Cylindrical Shell From Univorm Radial Impulse," *Proceedings of Fourth U. S. National Congress of Applied Mechanics*, University of California, Berkeley, Calif., June 18, 1962.

2 Anderson, D. L., and Lindberg, H. E., "Dynamic Pulse Buckling of Cylindrical Shells Under Transient Lateral Pressures," *AIAA Journal*, Vol. 6, No. 4, Apr. 1968, pp. 589-598.

3 Florence, A. L., "Buckling of Viscoplastic Cylindrical Shells Due to Impulsive Loading," *AIAA Journal*, Vol. 6, No. 3, Mar. 1968, pp. 532-537.

4 Florence, A. L., and Goodier, J. N., "Dynamic Plastic Buckling of Cylindrical Shells in Sustained Axial Compressive Flow," JOURNAL OF APPLIED MECHANICS, Vol. 35, No. 1, TRANS. ASME, Vol. 90, Series E, Mar. 1968, pp. 80-86.